Published in final edited form as:
Chem Commun (Camb). 2011 July 28; 47(28): 7977–7979. doi:10.1039/c1cc12933c.

In Vivo Cell Death Mediated by Synthetic Ion Channels

Bryan A. Smith[b], **Megan M. Daschbach**[d], **Seth T. Gammon**[a], **Shuzhang Xiao**[b], **Sarah E. Chapman**[b], **Caroline Hudson**[b], **David Piwnica-Worms**[a], **George W. Gokel**[d], and **W. Matthew Leevy**[b]

[a]Molecular Imaging Center, Mallinckrodt Institute of Radiology, Washington University School of Medicine, Campus Box 8225, St. Louis, MO 63110

[b]Department of Chemistry and Biochemistry, University of Notre Dame Notre Dame, IN 46556

[c]Freimann Life Science Center, University of Notre Dame Notre Dame, IN 46556

[d]Center for Nanoscience and Department of Chemistry and Biochemistry, University of Missouri St. Louis, One University Boulevard, St. Louis, MO 63121

The origins of supramolecular chemistry lie in crown ether and cryptand binding of alkali metals[1] and of other metals by cyclams,[2] but these early applications quickly led to a huge surge of structures.[3] When the structural types became extremely diverse, new applications emerged. Both structures and applications have increased in complexity and sophistication during the past four decades.[4] Currently, supramolecular systems are even used *in vivo* to mimic biological processes.[5] In this communication, we show that two offshoots, synthetic ion transporters and novel optical imaging compounds, of the original supramolecular concepts, can be used together in a live mouse to elicit acute tissue cell death and to monitor the process.

Direct injection, also called percutaneous injection, of chemotherapeutic agents involves the localized transfer of a drug into a target tissue using either a needle or catheter.[6] For shallow tissues, the injection may be guided by eye, but in deeper tissues the needle is often guided by sophisticated imaging technology.[7] This approach is advantageous for drugs that have either poor pharmacokinetics or broad toxicity, but still possess a therapeutic benefit. Examples include botulin toxin (BOTOX®) and both ethanol[8,9] and acetic acid,[10] which have seen clinical use for cancer treatment. Another clinical example is localized injection of sclerosing agents such as ethanolamine oleate for the treatment of varicose veins.[11] The direct injection of virus particles into tumors[12] is an emerging area as demonstrated by the recent report of intratumoral inoculation of a virus expressing mutant Na^+ channels.[13] These channels disrupted ion homeostasis in infected cancer cells, leading to tumor toxicity. The latter study confirmed that ion balance in cancer cells is a viable target for therapeutic agents.

Hydraphiles[14] are synthetic channel compounds[15] that insert in phospholipid bilayers and transport Na^+ cations through it. Several synthetic ion channel compounds are biologically active, and show antibacterial[16] or more general toxic behavior.[17] Although the therapeutic index for many of these compounds is not appropriate for therapies using oral or intravenous administration, they may be effective when applied by direct injection for non-invasive excision (ablation) of tissue. The hydraphiles exhibit broad toxic activity to bacteria, such as *Escherichia coli* and *Staphylococcus aureus*, to non-transformed mammalian cells including

Proofs to: G. W. Gokel, Ph.D. Department of Chemistry & Biochemistry, University of Missouri – Saint Louis, One University Boulevard, Saint Louis, MO 63121 USA, Telephone: 314-516-5321, Fax: (314) 516-5342, gokelg@umsl.edu.

HEK 293 and to cancerous CaCo2 cell lines. The toxicity of hydraphiles is linked to their ionophoretic activity. Specifically, these compounds insert into the plasma membrane and disrupt cellular ion gradients, inducing cell death. Hydraphiles **1** and **2** are shown below.

Compound **4** is a molecular probe for anionic phospholipids. Probe **4** incorporates two dipicolylamine-zinc(II) (DPA-$Zn2^{+}$) coordination complexes linked to a near-infrared (NIR) carbocyanine fluorophore (Cy7, λ_{exc} 794 nm, λ_{emit} 810 nm). Probe **4** has an affinity for anionic phospholipids such as phosphatidylglycerol (PG),[18] which is ubiquitous in bacteria, or phosphatidylserine (PS),[19] the primary anionic phospholipid found in mammalian membranes. Fluorophores such as **4** with emission wavelengths in the near infrared are optimal for *in vivo* studies because their spectral properties are minimally obscured by tissue.[20]

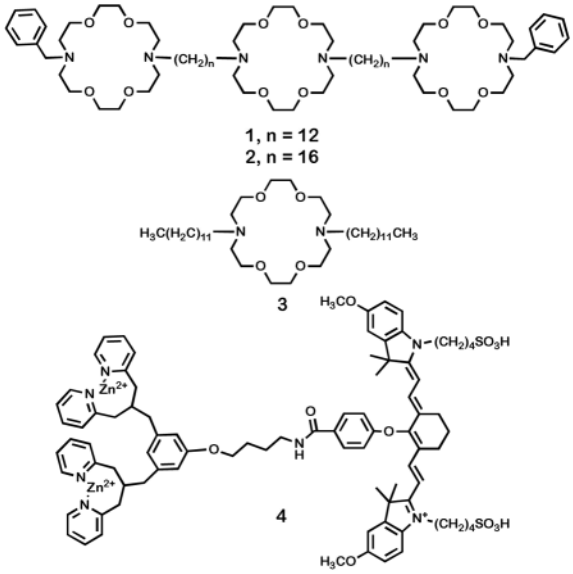

Previous studies using probe **4** demonstrated its ability to bind and image anionic phospholipids in animals. Thus, intravenous injection of **2** into living mice revealed the anionic PG lipids present on the surface of invading *Staphylococcus aureus* cells.[21,22] Phosphatidylserine, which is also bound by the DPA-Zn^{2+} affinity group,[23] is expressed on the inner leaflet of the mammalian plasma membrane. It remains essentially hidden, leaving the exterior cell surface charge neutral until cell death (apoptosis or necrosis) causes PS to flip or diffuse to the membrane surface where it can be detected by externally applied **2**.[24,25,26] We demonstrate below that **4** is useful for direct observation of *in vivo* tissue damage.

Hydraphiles are non-rectifying ion channels. Thus, when they insert into liposomal or cellular bilayers, they disrupt the ionic balance. From the high hydrophobicity of **1** (log P > 10),[27] we anticipated that membrane insertion would rapidly occur proximate to the site of direct injection and that diffusion and damage to surrounding healthy tissue would be minimal. While tumor sites are obvious targets for this approach, here we utilize a highly controlled system to elicit cell damage by **1** in mouse muscle tissue and subsequently to image the changes by using **4**.

In order to establish that rapid tissue damage would be selectively induced by a high concentration of synthetic channel, a model study was conducted via light microscopy using compounds **1 – 3** with HeLa cells. Compounds **1** and **2** are designed to be complete

hydraphile channels. The LC_{50} values for **1** to cultured HEK 293 and CaCo2 cells were previously reported as 2 μM and 12 μM, respectively, after 24 h.[17] To elicit rapid cell death, a concentration of 80 μM was used as it vastly exceeded the LC_{50}. However, at these levels, toxicity could even result from non-specific or other ion transport effects from alkly substituted crown ethers. Thus, compound **3,** the central fragment of **1**, was also tested. It is a known ion carrier, as opposed to a channel, and has much lower ion transport than **1** and **2**.[28] This initial study sought to demonstrate the importance of ionophoretic activity for cell death, even at very high concentrations. Figure 1 shows phase contrast microscopic images of HeLa cells that were treated with **1, 2,** and **3** at a concentration of 80 μM. The top row (panels A–C) shows the cells immediately after addition of **1, 2**, and **3**, respectively. Panels D–F show the cell status after 20 min. The cells treated with **1** are fully deformed and detached, while those treated with **2** show significant bulging of the plasma membrane (blebbing) and deformation. Cells treated with **3** showed minor blebbing relative to **1** and **2.** These changes in cell morphology are consistent with cell death.[29] These results confirmed that both **1** and **2** were lethal to HeLa cells after only 20 minutes, while **3** was less effective on the same time scale. At a concentration of 80 μM, both **1** and **2** would therefore be expected to have a localized and strongly toxic effect on vital tissue. We subsequently tested **1** as a representative hydraphile for in vivo studies.

Once the rapid toxic effect of **1** at a high concentration was established in HeLa cells, the combination of **1** and **4** as toxin and probe was evaluated in mice. Six nude mice (strain Nu/Nu, Taconic Inc.) were studied as follows. First, the animals were anesthetized and given an intramuscular (IM) injection of **1** (50 μL, 8 mM in EtOH) in the left rear leg muscle. Each animal also received a control injection (EtOH, 50 μL) in the right rear leg muscle. The animals were then returned to their cages for a 2 h incubation period, and subsequently injected intravenously (IV) with probe **4** (75 μL of a 1 mM aqueous stock).

Immediately after the injections of **1** and EtOH, the animals awoke from anesthesia. Visual observation showed that all six animals had no motor control over either hind leg, with both limbs appearing limp. At 6 h after injection of probe **2** (8 h post injection of **1**), the animals appeared to regain motor control of the EtOH injected limb: they would place body weight on the right leg while they nested, groomed, or ate. The animals regained little to no motor control of the hydraphile injected leg during the 21 h course of the experiment. This observation confirmed the biological activity of **1** in living mice.

Whole animal fluorescence imaging (Kodak In Vivo FX instrument, near infrared filter set optimized for Cy7) was performed to non-invasively monitor tissue damage caused by **1**. The animals were imaged at 6, 12, and 21 h post fluorophore injection. Figure 2 displays the time course of images from one mouse of the cohort that received the IM injection of hydraphile **1**, followed 2 h later by IV injection of **2**. Frame C shows the animal at 6 h post injection of **2**. No difference is apparent between the target (T) site injected with **1**, and the non-target (NT) site injected with EtOH (Figure 2, panel B). Since EtOH is itself toxic, we reasoned that some uptake of **2** would be noted in the control leg and that damage resulting from **1** might require additional time to resolve. A clear difference between injected and control legs was observed at the 12 h time point (panel D). The left-leg contrast apparent in panels D and E increased over time and the greatest difference was noted at the experiment's termination (21 h).

Figure 3 presents images for a cohort of three animals at the 21 h time point. Considerable fluorescence emission (from **4**) is apparent in the hydraphile-injected (left) leg but little is observed in the right leg (EtOH control). A control cohort (injected with **1** and a probe with no DPA-Zn(II) targeting moiety) showed no appreciable fluorescence. The results were

confirmed by conducting a duplicate experiment (different day, new cohort of mice, different solutions of **1** and **4**).

The trends apparent in the images were confirmed by a quantitative analysis. Mean pixel intensities were determined for four regions of interest: target (T), non-target (NT), liver (L), and abdomen (ABD). Table I presents the average fluorescence ratios of T/NT, T/L, and T/ABD, reported with the standard error of the mean (SEM). The T/NT ratio is a direct measure of the uptake of **4** at the hydraphile site compared to the contralateral (right leg) EtOH control (NT). The T/L and T/ABD ratios are a measure of the relative intensity at the target site compared to the rest of the animal as the probe is excreted and/or metabolized. During the first 6 h of the experiment, injury sites were poorly distinguished: all three measures of fluorescent probe accumulation were close to unity. However, after another 6 h (*i.e.* after 12 h) contrast was sufficient that the ratios increased as follows: T/NT, 1.73; T/L, 1.76; and T/ABD, 2.17. Panel D of Figure 2 confirms the contrast between injured (left) and control legs at 12 h. The T/NT and T/ABD ratios were essentially unchanged for the remainder of the experiment, but the T/L ratio did increase, indicating that probe continued to clear from the animal. For experiments using fluorescent probe control **3**, each of these three ratios had values ≤ 1 for the entire time course of the experiment.

A histological study was conducted on nine mice to compare and contrast the effects of **1** and EtOH. The mice were injected IM with **1** and EtOH as described above. After 24 h the muscle tissues were extracted, fixed, and stained for histological analysis. Mouse muscle tissue injected with **1** showed severe acute inflammation and other morphological effects (data not shown). This contrasted with the tissue from EtOH-injected tissue, which showed less severe effects by all criteria. These histology experiments provide additional data that confirm the tissue damage caused by injection of **1** into living muscle tissue. As such, it confirms the potential application of **1** as an anti-tumor agent if administered by direct injection.

Direct injection is a clinically important strategy for localized delivery of chemotherapeutic agents. This approach is used with many agents in tumor ablation therapy. We demonstrate in the work reported here that synthetic ionophore **1**, although too toxic for non-targeted application, may hold significant potential as a direct injection agent. The ability of **1** to attack tissue in a localized fashion by direct injection has been confirmed by using near-infrared probe **4** in combination with histological analysis. Compounds **1** and **4** represent a merger of biomimetic and sensor branches of supramolecular chemistry in an application of potential clinical value.

Acknowledgments

We thank the NIH (grant GM075762 and P50 CA94056), the Walther Cancer Center, the NSF (CHE-0957535) and the Notre Dame Integrated Imaging Facility for funding support.

References

1. (a) Pedersen CJ. Cyclic polyethers and their complexes with metal salts. J Am Chem Soc. 1967; 89:7017–36.(b) Dietrich B, Lehn JM, Sauvage JP. Diaza-polyoxa-macrocyclic and macrobicyclic compounds. Tetrahedron Lett. 1969; 1969:2885–2888.
2. Liang X, Sadler PJ. Chem Soc Rev. 2004; 33:246–266. [PubMed: 15103406]
3. (a) Gokel, GW.; Korzeniowski, SH. Macrocyclic polyether syntheses. Springer-Verlag; Berlin: 1982. p. 410(b) Bradshaw, JS.; Krakowiak, KE.; Izatt, RM. Aza-Crown Compounds. Vol. 51. Wiley; New York: 1993. p. 885
4. Steed, JW.; Atwood, JL. Supramolecular Chemistry. 2. John Wiley & Sons, Ltd; Chichester: 2009.

5. (a) Leevy WM, Huettner JE, Pajewski R, Schlesinger PH, Gokel GW. Synthetic Ion Channel Activity Documented by Electrophysiological Methods in Living Cells. J Am Chem Soc. 2004; 126:15747–15753. [PubMed: 15571397] (b) Pajewski R, Garcia-Medina R, Brody SL, Leevy WM, Schlesinger PH, Gokel GW. A synthetic, chloride-selective channel that alters chloride transport in epithelial cells. Chem Commun. 2006:329–31.
6. Oldham, RK.; Dillman, RO., editors. Principles of Cancer Biotherapy. 5. Springer; New York: 2009. p. 744
7. Gillams AR. Cancer Imaging. 2005; 5:103–109. [PubMed: 16305946]
8. Van de Pulte M, Wang H, Chen F, de Wilte PA, Ni Y. Acad Radiol. 2008; 15:107–113. [PubMed: 18078913]
9. Koda M, Murawaki Y, Mitsuda A, Ohyama K, Horie Y, Suou T, Kawasaki H, Ikawa S. Cancer. 2000; 88:529–537. [PubMed: 10649243]
10. Minowada S, Fjuimura T, Takahashi N, Kishi H, Hasuo K, Minami M. J Clin Endocrin & Metab. 2003; 88:5814–5817.
11. Tisi PV, Beverly C, Rees A. Cochrane Database of Systematic Reviews. 2006; 18:CD001732.
12. Stewart AK, Lassam NJ, Quirt IC, Bailey DJ, Rotstein LE, Krajden M, Dussureault S, Gallinger S, Cappe D, Wan Y, Addison CL, Moen RC, Gauldie J, Graham FL. Gene Ther. 1999; 6:350–363. [PubMed: 10435085]
13. Tannous BA, Christensen AP, Pike L, Wurdinger T, Perry KF, Saydam O, Jacobs AH, Garcia-Anoveros J, Weissleder R, Sena-Esteves M, Corey DP, Breakefield XO. Mol Ther. 2009; 17:810–9. [PubMed: 19259066]
14. Gokel GW. Chem Comm. 2000:1–9.
15. Fyles TM. Chem Soc Rev. 2007; 36:335–47. [PubMed: 17264934]
16. Fernandez-Lopez S, Kim HS, Choi EC, Delgado M, Granja JR, Khasanov A, Kraehenbuehl K, Long G, Weinberger DA, Wilcoxen KM, Ghadiri MR. Nature. 2001; 412:452–5. [PubMed: 11473322]
17. (a) Leevy WM, Donato GM, Ferdani R, Goldman WE, Schlesinger PH, Gokel GW. J Am Chem Soc. 2002; 124:9022–3. [PubMed: 12148985] (b) Leevy WM, Gammon ST, Levchenko T, Daranciang DD, Murillo O, Torchilin V, Piwnica-Worms D, Huettner JE, Gokel GW. Org Biomol Chem. 2005; 3:3544–3550. [PubMed: 16172693]
18. Leevy WM, Johnson JR, Lakshmi C, Morris J, Marquez M, Smith BD. Chem Commun. 2006:1595–1597.
19. Lakshmi C, Hanshaw RG, Smith BD. Tetrahedron. 2004; 60:11307–11315.
20. Bashkatov AN, Genina EA, Kochubey VI, Tuchin VV. J Phys D: Appl Phys. 2005; 38:2543–2555.
21. Leevy WM, Gammon ST, Jiang H, Johnson JR, Maxwell DJ, Jackson EN, Marquez M, Piwnica-Worms D, Smith BD. J Am Chem Soc. 2006; 128:16476–16477. [PubMed: 17177377]
22. Leevy WM, Gammon ST, Johnson JR, Lampkins AJ, Jiang H, Marquez M, Piwnica-Worms D, Suckow MA, Smith BD. Bioconjugate Chem. 2008; 19:686–692.
23. Koulov AV, Stucker KA, Lakshmi C, Robinson JP, Smith BD. Cell Death and Differentiation. 2003; 10:1357–1359. [PubMed: 12970674]
24. Hanshaw RG, Smith BD. Bioorg Med Chem. 2005:5035–5042. [PubMed: 15914007]
25. Hanshaw RG, Lakshmi C, Lambert TN, Johnson JR, Smith BD. Chembiochem. 2005; 6:2214–2220. [PubMed: 16276499]
26. Yang SK, Attipoe S, Klausner AP, Tian R, Pan D, Rich TA, Turner TT, Steers WD, Lysiak JJ. J Urol. 2006; 176:830–835. [PubMed: 16813956]
27. Murillo O, Suzuki I, Abel E, Murray CL, Meadows ES, Jin T, Gokel GW. J Am Chem Soc. 1997; 119:5540–5549.
28. Leevy WM, Weber ME, Gokel MR, Hughes-Strange GB, Daranciang DD, Ferdani R, Gokel GW. Org Biomol Chem. 2005; 3:1647–52. [PubMed: 15858645]
29. Zieger U, Groscurth P. News Physiol Sci. 2004; 19:124–128. [PubMed: 15143207]

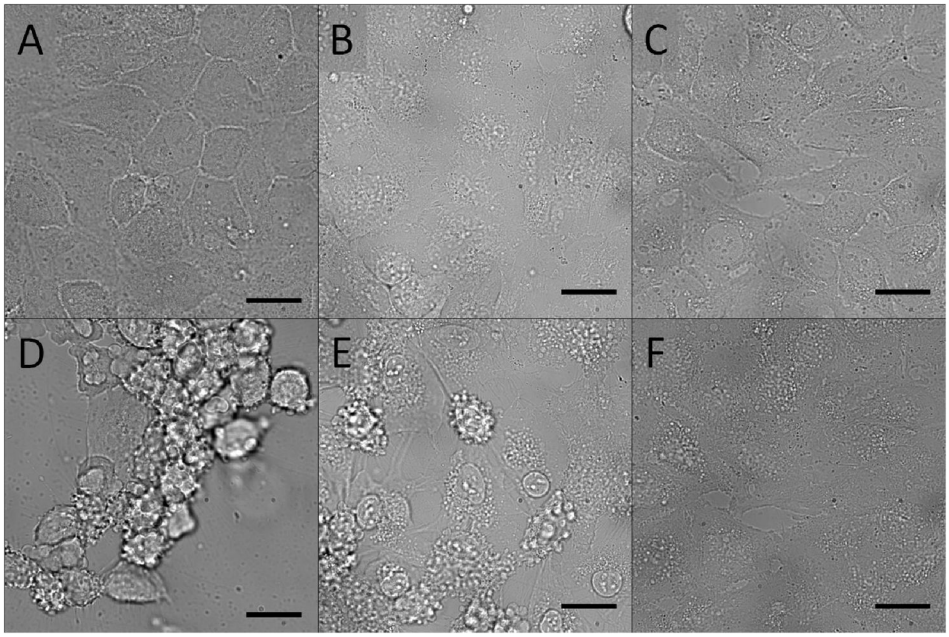

Figure 1.
Phase contrast images of HeLa cells recorded at t = 5 sec (A–C) and t = 20 min (D–F) post treatment with 80 μM of **1** (A, D), **2** (B, E), and **3** (C, F) Scale bar = 10 μm.

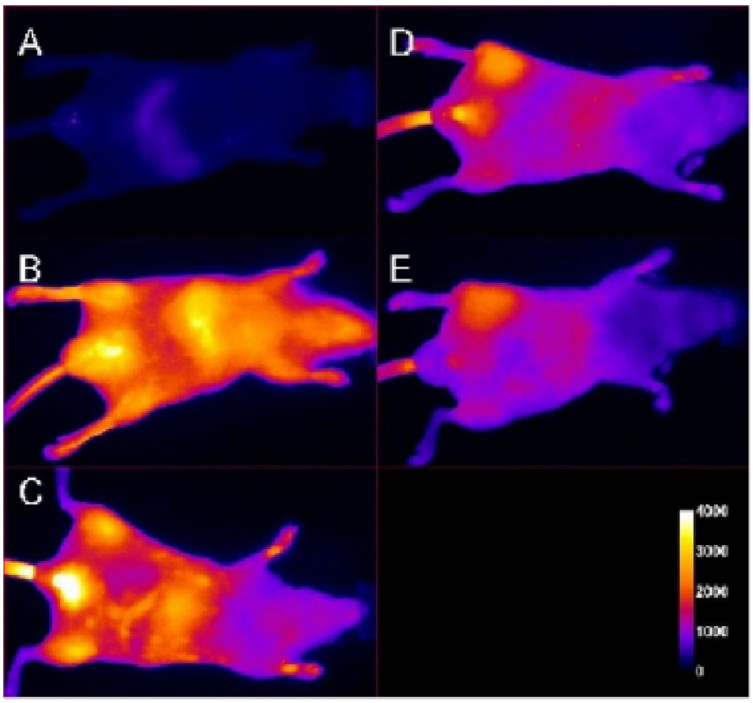

Figure 2.

Fluorescence images of a mouse before (A) and immediately after (B) IV injection of **2**. The mouse received 50 μL IM injections of **1** (10 mM stock solution, left leg) and EtOH (right leg) 2 h prior to administration of **4**. Panels C, D, and E show the mouse at 6 h, 12 h, and 21 h post injection of **4**.

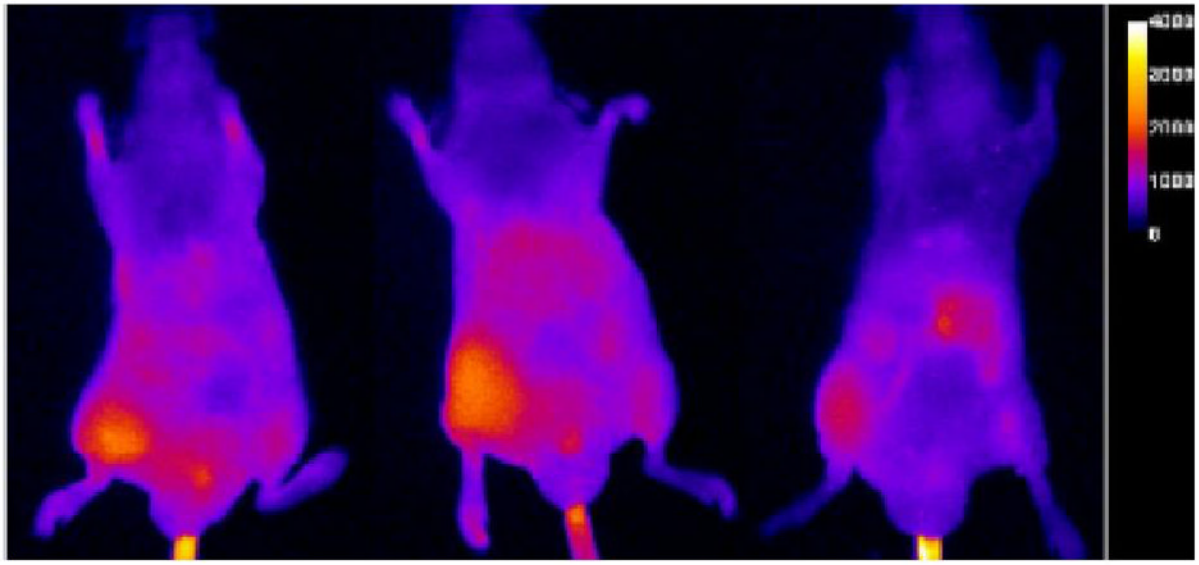

Figure 3.
Fluorescent images of mice injected IM with **1** (left leg) and EtOH (right leg). Fluorescent probe **4** was injected IV 2 h later. The images shown were taken 21 h after injection of **4**.

Table 1

Mean fluorescence ratios (± SEM) of the Target (T) to Non-Target (NT), Liver (L), and Abdomen (ABD) sites at times 0, 6, 12, and 21 h post injection of **2**.

	Mean fluorescence ratios		
Time (h)	**T/NT**	**T/L**	**T/ABD**
0	1.18 ± 0.06	0.75 ± 0.05	1.27 ± 0.11
6	1.25 ± 0.19	1.09 ± 0.06	1.47 ± 0.23
12	1.73 ± 0.03	1.76 ± 0.11	2.17 ± 0.04
21	1.74 ± 0.08	2.04 ± 0.28	1.97 ± 0.09